Proceedings World Geothermal Congress 2000
Kyushu - Tohoku, Japan, May 28 - June 10, 2000

MODELLING THE EVOLUTION OF GRANITE PERMEABILITY AT HIGH TEMPERATURE

Sutopo [1,3], Stephen P. White [2], Norio Arihara [1]
[1]Waseda University, 3-4-1 Okubo Shinjuku-ku, Tokyo, Japan
[2]Applied Mathematics, N.Z. Institute for Industrial Research and Development, PO Box 31-310, Lower Hutt, New Zealand
[3]Bandung Institute of Technology (ITB), Jl Ganesha 10 Bandung, Indonesia

Key Words: CHEM-TOUGH2, chemical modelling, deposition, granite, permeability evolution

ABSTRACT

In this paper we describe modelling the complicated processes of mineral deposition/dissolution in porous or fractured rock at high temperatures. The effect of this process on the evolution of permeability and porosity within the rock is calculated. A numerical model was constructed using CHEM-TOUGH2 to simulate a recent experimental study of permeability changes in Westerly granite. As cementation proceeds, surface area available for deposition is modified, inducing changes in the kinetic deposition rate. In order to model this feedback effect adequately, we included a correlation between surface area and porosity. These results are compared to the measured permeability and flowrate changes over time in the granite core flood experiments of Moore *et al*. The temperature range of the experiments was 300 – 500^o C. Model predictions match the experimental permeability and flowrate curves quite well at late time with less than 10% error in all cases. In some cases the match to early time data is not so good with errors up to 30% in some cases.

1. INTRODUCTION

Flow of fluids through the Earth's crust is fundamentally controlled by permeability that, in crystalline rocks, is primarily controlled by interconnected networks of cracks. In hydrothermal settings, it has long been believed that precipitation of silica and other minerals at shallow levels clogs permeable pathways and may seal off sections of the systems.

In several laboratory experiments a heated aqueous fluid was passed through a rock sample down an applied temperature gradient. These demonstrated that the permeability of granite decreases substantially with time in such cases (Morrow *et al*., 1981; Moore *et al*., 1983; and Vaughan *et al*., 1986).

Recently, Weir and White (1996) and White and Mroczek (1998) calculated the rate of change in porosity and permeability due to dissolution and precipitation of quartz. In these calculations only the silica reaction was considered.

In this paper we construct a numerical model of the experiments of Moore *et al*. (1995) on Westerly granite at high temperature and pressure using the reactive transport simulator CHEM-TOUGH2. With this model we calculate the changes in flowrate and permeability that result from complicated reactions taking place in the experiment.

2. LABORATORY EXPERIMENTS

Moore *et al*. (1994 and 1995) conducted several experiments on Westerly granite under hydrothermal conditions in an effort to understand the evolution of permeability over time of rock and gouge materials as a function of temperature. Parameters related to the Moore *et al*. (1995) experiments are given in Table 1.

They conducted all the experiments at temperatures between 300^o and 500^o C, with a confining pressure of 150 MPa and a pore pressure of 100 MPa. The pore fluid was initially de-ionized water. During the experiment, the pump was set to maintain the pore pressure on one side of the sample at a fixed value, up to 2.0 MPa above the pressure on the other side. This produced a steady-state flow through the sample. The high and low pore pressure sides were reversed periodically during each experiment (see Fig. 1) to measure permeability in both directions and to keep the same fluid in contact with the sample. This meant the same small volume of water was continually pushed back and forth through the sample.

Most of the experiments were conducted on an intact cylinder of Westerly granite, but one configuration at 400^o C fractured in tension parallel to the axis was also tested. This was to simulate a fracture in the country rock adjacent to a fault zone. One configuration consists of a layer of granite gouge sandwiched between granite end-pieces used to determine the effect of fault gouge on the rate of permeability change.

These experiments found that the permeability of Westerly granite in the temperature range 300^o to 500^o C decreased with time during these experiments. They speculated the rapid initial decreases in all of the experiments might reflect a combination of thermal and fluid equilibration processes. Their analysis showed that the permeability reductions are caused by a combination of solution transfer processes and metamorphic reactions. Their results suggested the rate of permeability reduction increases irregularly with increasing temperature, perhaps reflecting changing mineral reactions. They found that intact granite cylinders tested at 500^o C showed a rapid drop in permeability after 5 to 6 days, to the extent that flow through one rock cylinder essentially ceased. They suggested that the cause of this precipitous decrease might be crack healing.

The experiments showed that the permeability of samples containing a layer of granite gouge decreased at more rapid rates over the first 10–14 days than they did for equivalent intact samples. They suggested that preferential dissolution and re-deposition of a finite amount of extremely fine-grained gouge might cause the rapid initial decreases in permeability.

3. CHEMICAL MODELLING

3.1 Thermodynamic Data

Moore *et al*. (1995) describe the Westerly granite used in these experiments as a granodiorite consisting principally of plagioclase (~40%), quartz (~25%), K-feldspar (~25%) and biotite (~5%). For the numerical modelling described here we treat this as a porous media consisting of the minerals given in Table 2. The chemical formulae of the mineral reactions are given in Table 3.

There is reasonable data on reaction rates and equilibrium constants describing the dissolution and precipitation of quartz at the temperatures and pressures used in the experiments of Moore *et al.* (1995). The most comprehensive compilation is probably that of Dove (1994) and we have used the expression for reaction rate derived in his paper for our work. Manning (1994) has reviewed all the solubility data for quartz and derived an expression for the solubility of quartz of the form

$$\log(K) = A + \frac{B}{T} + \frac{C}{T^2} + \frac{D}{T^3} + \left[E + \frac{F}{T} + \frac{G}{T^2}\right]\log(\rho_{H_2O}) \quad (1)$$

where the coefficients *A*-*G* are listed in Table 4.

Unfortunately there is much less information available about the other minerals composing the granite. While data is available at temperatures below 350° C, very little is available above this temperature. Also, much of this data lacks any information as to the effect of pressure, and we believe this is crucial for the understanding of these experiments. For these reasons we used the computer program SUPCRT92 (Johnson *et al.,* 1992) to calculate equilibrium constants for the dissolution of the other minerals as functions of temperature and pressure. For convenience in modelling, we derived correlations to the tabulated data from SUPCRT92 of the form

$$\log(K) = \sum_{i=1}^{5} a_i T^{i-1} + (a_6\tau + a_7\tau^2)P' \quad (2)$$

where T is the temperature in °C, $\tau = (T - 300)$, $P' = (P - 9.0\times10^7)/1.0\times10^8$, and P is the pressure in Pa. The values for the coefficients a_i are given in Table 5. A warning must be given that these correlations are valid only over the pressure and temperature ranges of the experiments ($250 < T < 500$), ($9.0\times10^7 < P < 1.0\times10^8$). They are not claimed to cover a significant part of P, T space. The dissociation constant for water was treated in the same manner although in this case there was no need to allow for pressure dependence.

As no data on kinetic reaction rates other than for quartz was available at the pressures and temperatures of the experiments, we assumed equilibrium for all minerals other than quartz.

3.2 Modelling Software

For this work we have used a version of TOUGH2 (Pruess, 1991) that has been modified to include the transport of reacting chemicals (White, 1995). The original code was capable of modelling temperatures up to 350° C and pressure up to 100 MPa. This has been extended to temperatures up to 800° C, but the pressure limit of 100 MPa remains (White and Mroczek, 1998).

We have added a new type of `SOURCE` to the `GENER` block called `PRES`. This sets the pressure of specified elements to the value set for the production rate of source.

3.3 Description of Numerical Model

A one-dimensional model was developed for simulating the decreasing permeability of granite experiment. It consists of 50 grid blocks with a constant spacing along the core axis (21.9 mm long and 19.1 mm in diameter), and two inactive elements at the end of the core, by which we can set the pressure in the boundary elements at fixed times (Fig. 1).

Initial permeability is the same as the initial heated permeability data of Moore *et al*. (Table 1). The porosity was adjusted to obtain a match to the observed reduction of permeability and flowrate. The surface area of rock available for interaction with the fluid is calculated from a correlation function of porosity (Darot *et al*., 1992; White and Mroczek, 1998), and then modified by the amount of quartz in the granite. For example, if 20 % of the granite is quartz, then the surface area of quartz was simply assumed to be 20% of the total surface area.

4. RESULTS AND DISCUSSION

4.1 Calculating *k*

Moore *et al*. (1995) experimentally determined the permeability of the intact and sandwich samples by measuring the fluid flux at interval over a constant pressure gradient, and by applying Darcy's law as

$$k_{av} = \frac{\mu}{\rho}\frac{Q}{A}\left(\frac{L}{P_2 - P_1}\right) \quad (3)$$

where Q is flow rate in kg/sec, k_{av} the average permeability, μ the viscosity, L the length of the sample, P_2 and P_1 the pressure at the ends of the sample, A the area of the sample and ρ the fluid density. In the numerical modelling we calculate k in each element. The effective modelled value of k is given by the harmonic mean of k in each element (provided each element is the same size).

$$\frac{1}{k_{eff}} = \frac{1}{N}\sum_{elements}\frac{1}{k_i} \quad (4)$$

where N is the number of elements.

4.2 Results

In this work we attempted to quantify the permeability reducing activity in the granite core from 13 intact samples and two granite gouge samples of Moore *et al*. (1995). They did not measure an initial porosity, and there is considerable uncertainty in the porosity of granite and the state of silica content within the samples. We therefore adjusted the initial porosity and initial silica concentration as matching parameters to get the best fit to the data. It has been suggested by Morey *et al*. (1962) that very fine quartz particles are many times more soluble than normal quartz crystals. The effect seems to be well established but is not well enough quantified to include fully in the modelling. Using different initial aqueous concentrations of silica was a crude attempt to include the effect of such fines in the numerical modelling. The fines would rapidly dissolve due to a very large ratio of surface area to volume giving a solution supersaturated with respect to quartz. We calculated the average permeability using Eq. (4) and flowrate as a function of time, and compared the result with experimental data. We have found

that the values of matching porosity are in the range 0.4035 – 2.6933 % which is quite close to that of Morrow and Lockner (1997). Their measurements of permeability and porosity on granite cores are in the range 0.52 – 1.36 %. The values of initial concentration of SiO_2 (aq) used for matching permeability reduction are given in Fig. 2. As observed, there exists correlation between initial concentration of silica and temperature.

Figs. 3 – 7 compare the numerical results with 13 experiments on the intact granite. Fig. 8 compares the numerical results with two experiments on gouge granite. Although agreement is not perfect at early times, generally they match very well to the experimental data at the later times. There are some experiments where good agreement could not be obtained for the rapid early drop in permeability. We suspect the rapid change in permeability at early times may be due to fines as suggested by Moore *et al*. (1995). If there was a small amount of quartz present in this form, then this would cause a rapid decrease in permeability until silica in this form was exhausted followed by slower dissolution/deposition of quartz that our modelling seems to match quite well.

5. MODELLED CHEMICAL CHANGES

For the run HTQP21 we looked in some detail at the chemical changes in the granite predicted by the numerical modelling. We considered two cases, in the first pure water was used as the initial pore fluid and in the second a 0.1 M NaCl brine was used. The results of the modelling are summarized in Table 6.

In both cases quartz is almost exclusively responsible for the change in permeability. Quartz is dissolved from near the ends of the cylinder and precipitates over most of the body of the cylinder. When Na^+ ions are present there is some conversion of k-feldspar to albite.

6. CONCLUSIONS

Case studies at various temperatures were carried out, and the comparisons of the predicted and measured permeability evolution during high-temperature fluid flow through granite core samples demonstrate that the model reproduces quite well the complicated processes of mineral deposition and dissolution.

The work suggests the mechanism responsible for permeability reduction is the dependence of quartz solubility on pressure. The effect of this is to dissolve quartz from the high-pressure end of the cylinder and precipitate quartz along the cylinder as fluid moves along the pressure gradient. There are significant changes in permeability at the ends of the cylinder when the flow is reversed but the net change over time is a reduction in permeability of the cylinder.

The effect of fines could have been modelled by regarding them as a separate mineral with a different solubility and reaction rate from quartz. However there is insufficient experimental data on what values should be adopted for these parameters to make this approach feasible at present.

ACKNOWLEDGMENTS

We thank D. E. Moore of U.S. Geological Survey for kindly supplying experimental data from their high temperature permeability experiment and to W.M. Kissling and E.K Mroczek for their critical reading of the manuscript and suggestions for improvement.

Table 1: Summary of experiments

REFERENCES

Darot, M., Gueguen, Y., and Baratin, M.L. (1992). Permeability of thermally cracked granite. *Geophys. Res. Lett.*, Vol.19(9), pp.869-872.

Dove P.M. (1994). The dissolution kinetics of quartz in sodium chloride solutions at 25° to 300° C. *American J. Sci.* Vol.294, pp.665–712.

Johnson, J.W., Oelkers, E.H., and Helgeson, H.C. (1992). A software package for calculating the standard molal thermodynamic properties of minerals, gases, aqueous species and reaction from 1 to 5000 bar and 0 to 1000° C. *Computer & Geosciences*, Vol. 18, pp.899-947.

Manning, C.E. (1994). The solubility of quartz in H_2O in the lower crust and upper mantle. *Geochim. Cosmochim. Acta*, Vol.58, pp.4831-4839.

Moore, D.E., Morrow, C.A., and Byerlee, J.D. (1983). Chemical reactions accompanying fluid flow through granite held in a temperature gradient. *Geochim. Cosmochim. Acta*, Vol.47, pp.445-453.

Moore, D.E., Lockner, D.A., and Byerlee, J.D. (1994). Reduction of permeability in granite at elevated temperatures. *Science*, Vol.265, pp.1558-1561.

Moore, D.E., Liu, L.Q., Lockner, D.A., Summer, R., and Byerlee, J.D. (1995). *High-Temperature Studies – 1. Permeability of Granite and Novaculite at 300° to 500° C*. U.S. Geol. Surv. Open-File Report 95-28, Menlo Park, CA, 79pp.

Morey, G.W., Fournier, R.O., Rowe, J.J. (1962). The solubility of quartz in water in the temperature interval from 25° to 300° C. *Geochim. Cosmochim. Acta*, Vol.26, pp.1029-1043.

Morrow, C., Lockner, D., Moore, D., and Byerlee, J. (1981). Permeability of granite in a temperature gradient. *J. Geophys. Res.*, Vol.86, pp.3002-3008.

Morrow, C., and Lockner, D. (1997). Permeability and porosity of the Illinois UPH 3 drillhole granite and a comparison with other deep drillhole rocks. *J. Geophys. Res.*, Vol.102, pp.3067-3075.

Pruess, K. (1991). *TOUGH2 – A General-Purpose Numerical Simulator for Multiphase Fluid and Heat Flow*. Report LBL-29400, Lawrence Berkeley Lab., Berkeley, CA. 102pp.

Vaughan, P.J., Moore, D.E., Morrow, C.A., and Byerlee, J.D. (1986). Role of cracks in progressive permeability reduction during flow of heated aqueous fluids through granite. *J. Geophys. Res.*, Vol.91, pp.7517-7530.

Weir, G.J. and White, S.P. (1996). Surface deposition from fluid flow in porous medium. *Transport in Porous Media*, Vol.25, pp.79-96.

White, S.P. (1995). Multiphase non-isothermal transport of systems reacting chemicals. *Water Resour. Res.*, Vol.31, pp.1761-1772.

White, S.P. and Mroczek, E.K. (1998). Permeability changes during the evolution of a geothermal field due to the dissolution and precipitation of quartz. *Transport in Porous Media*, Vol.33, pp.81-101.

All experiments were conducted at 150 MPa confining pressure and 100 MPa fluid pressure.

Experiment Number	Sample Configuration	Temperature (°C)	# Days Heated	*k*-room T* ($m^2 \times 10^{-21}$)	*k*-heated** ($m^2 \times 10^{-21}$)	
					initial	final
HTQP01	Intact novaculite	400	1.9	6856	12693.0	4146.0
HTQP02	Quartz gouge, novaculite end pieces	400	4.2	10817	13920.0	4368.0
HTQP03	Quartz gouge, granite end pieces	400	14.1	144	38.4	66.8
HTQP04	Granite gouge, granite end pieces	500	9.9	82	514.4	42.0
HTQP05	Intact granite	500	10.0	102	326.8	19.4
HTQP06	Intact granite	500	9.8	609	465.4	0.4
HTQP07	Intact granite	400	45.8	193	137.6	18.3
HTQP08	Granite gouge, granite end pieces	400	23.7	876	1230.9	171.8
HTQP09	Intact granite	450	0.3	309	211.6	179.2
HTQP10	Intact granite	450	19.5	1240	364.5	129.9
HTQP11	Intact granite	300	19.5	413	166.1	59.1
HTQP12	Intact granite	350	13.6	473	171.5	92.0
HTQP13	Intact granite	300	17.6	104	99.6	56.5
HTQP14	Tensile fracture in granite	400	27.8	-	-	(31.4)
HTQP15	Intact granite	350	12.9	63	213.1	122.4
HTQP16	Intact granite	350	19.1	103	170.0	91.5
HTQP17	Intact granite	450	0.1	489	326.4	273.3
HTQP18	Intact granite	450	20.0	466	404.0	121.4
HTQP19	Intact granite	400	9.9	348	234.1	136.4
HTQP20	Intact granite	400	5.9	99	197.6	136.8
HTQP21	Intact granite	400	31.9	71	139.6	38.6

***)** ***k*-room T**: room-temperature measurements of permeability
****)** ***k*-heated** : heated-temperature measurements of permeability

Table 2: Composition of granite used for numerical modelling.

Mineral	Albite	Anorthite	K-feldspar	Quartz	Annite (Biotite)
Mass fraction	22.5%	22.5%	25%	25%	5%

Table 3: Chemical reaction equations for OH^- and the mineral reactants

No	Mineral or OH^-	Reactions equation
1	OH^-	$OH^- + H^+ = H_2O$
2	Quartz	$SiO_2 = SiO_2\,(aq)$
3	K-feldspar	$KAlSi_3O_8 + 4\,H^+ = K^+ + Al^{+++} + 3\,SiO_2(aq) + 2\,H_2O$
4	Albite	$NaAlSi_3O_8 + 4\,H^+ = Na^+ + Al^{+++} + 3\,SiO_2(aq) + 2\,H_2O$
5	Anorthite	$CaAl_2Si_2O_8 + 8\,H^+ = Ca^{++} + 2\,Al^{+++} + 2\,SiO_2(aq) + 4\,H_2O$
6	Annite	$KFe_3AlSi_3O_{10}(OH)_2 + 10\,H^+ = K^+ + 3\,Fe^{++} + Al^{+++} + 3\,SiO_2(aq) + 6\,H_2O$

Table 4: Coefficients for Equation (1)

A	*B*	*C*	*D*	*E*	*F*	*G*
4.2620	-5764.2	1.7513E+6	$-2.2869 \times 10^{+8}$	2.8454	-1006.9	$3.5689 \times 10^{+5}$

Table 5: Coefficients used in Equation (2).

Mineral	a_1	a_2	a_3	a_4	a_5	a_6	a_7
Albite	11.67260	-0.1108710	0.355548×10^{-3}	-0.631207×10^{-6}	0.476326×10^{-9}	0.0300033	-0.207436×10^{-3}
Anorthite	41.38390	-0.2894990	0.843097×10^{-3}	-0.147705×10^{-5}	0.113016×10^{-8}	0.0573145	-0.459006×10^{-3}
K-feldspar	6.90926	-0.0886285	0.301236×10^{-3}	-0.561615×10^{-6}	0.438459×10^{-9}	0.0292632	-0.202774×10^{-3}
Annite	42.74250	-0.2562440	0.753660×10^{-3}	-0.131129×10^{-5}	0.995930×10^{-9}	0.0553072	-0.420283×10^{-3}

Table 6: Chemical changes in granite.

Mineral	Case 1 – Pure water	Case 2 – 0.1 M NaCl
Albite	Almost no change	Some precipitation
Anorthite	No change	Almost no change
K-feldspar	Almost no change	Some dissolution
Quartz	Dissolves from ends precipitates in body	Dissolves from ends precipitates in body
Annite	Almost no change	Almost no change

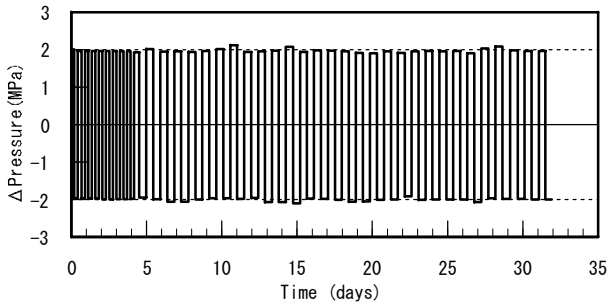

Fig.1: Differential pressure between the ends of the sample of HTQP21.

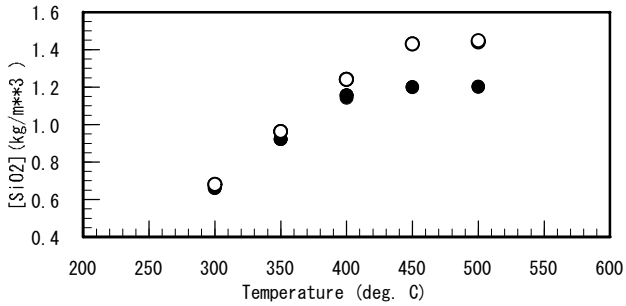

Fig. 2: Initial concentration of SiO_2 versus temperature ●: pore pressure 90 MPa o: pore pressure 100 Mpa.

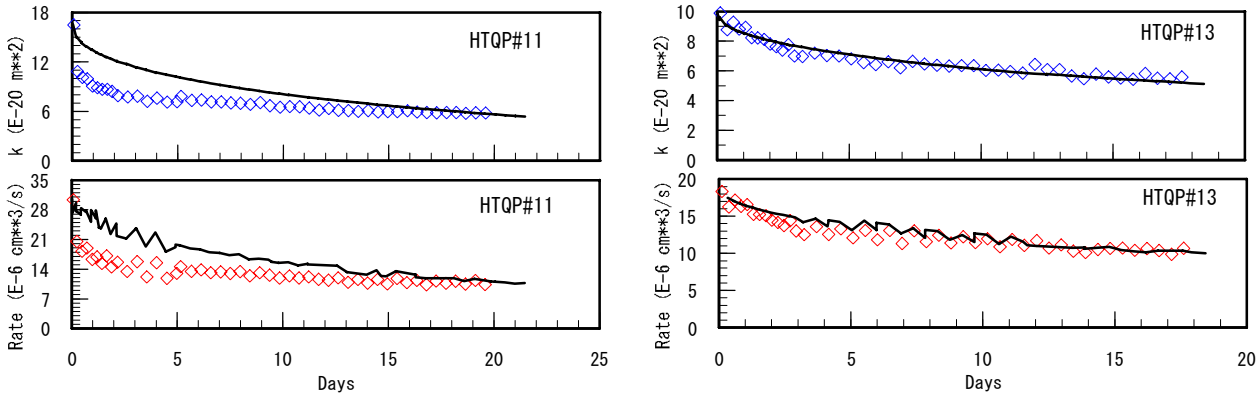

Fig. 3: Comparison between measured (symbols) and calculated (line) permeability and flowrate of intact granite at T=300º C.

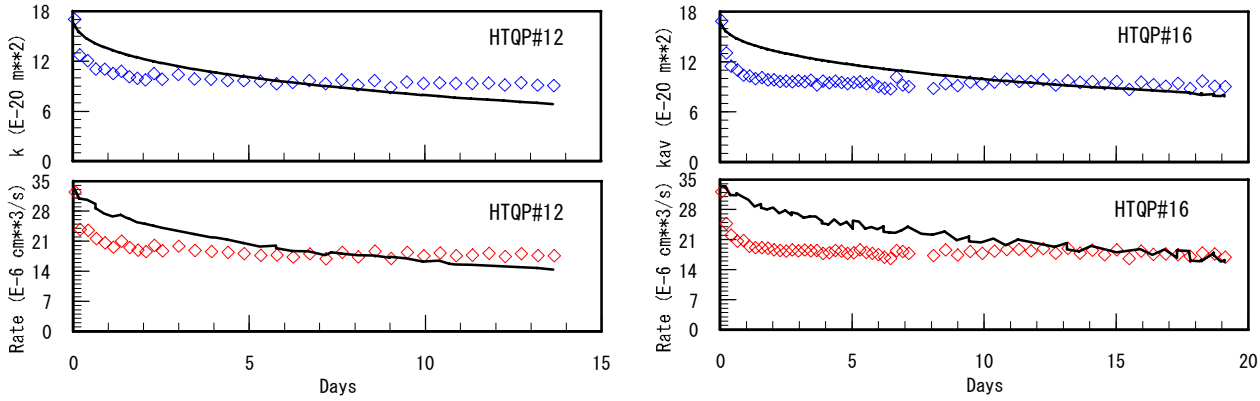

Fig. 4: Comparison between measured (symbols) and calculated (line) permeability and flowrate of intact granite at T=350º C.

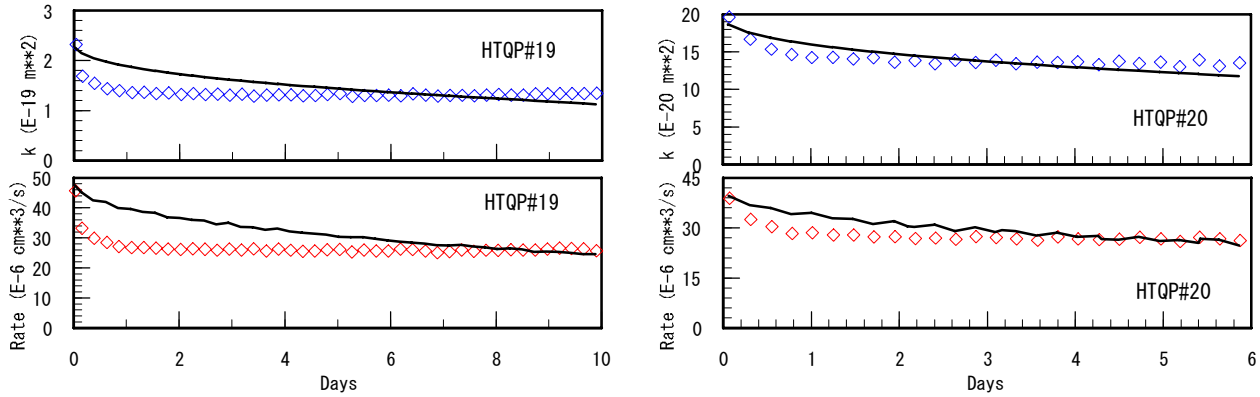

Fig. 5: Comparison between measured (symbols) and calculated (line) permeability and flowrate of intact granite at T=400º C.

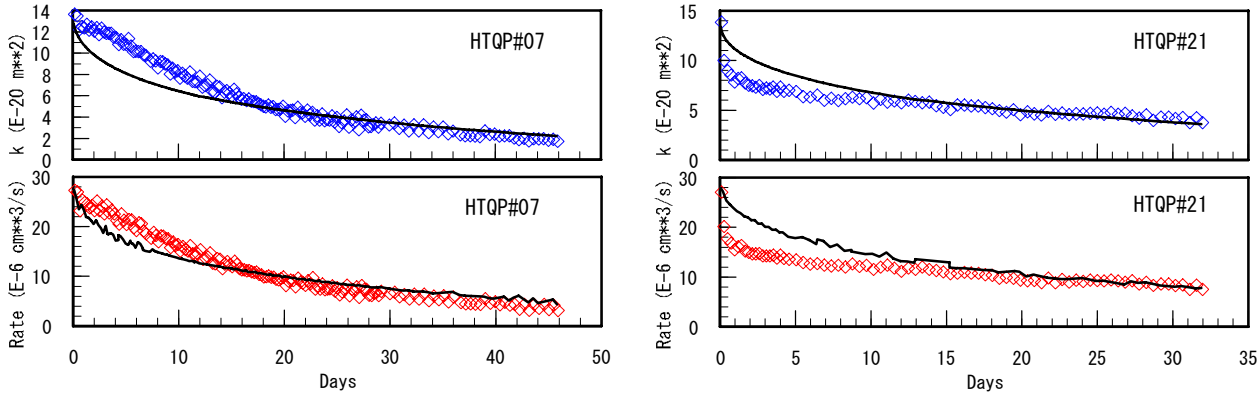

Fig. 5a: Comparison between measured (symbols) and calculated (line) permeability and flowrate of intact granite at T=400º C.

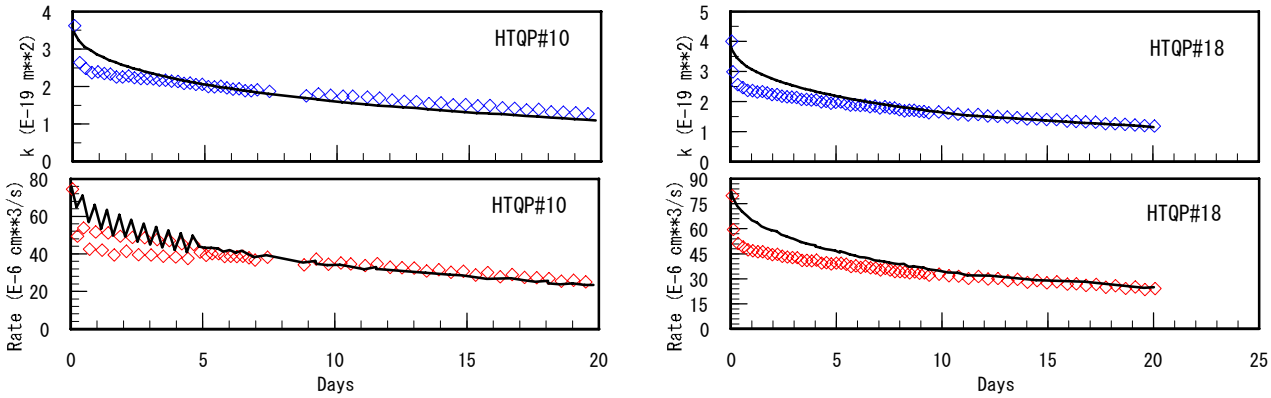

Fig. 6: Comparison between measured (symbols) and calculated (line) permeability and flowrate of intact granite at T=450º C.

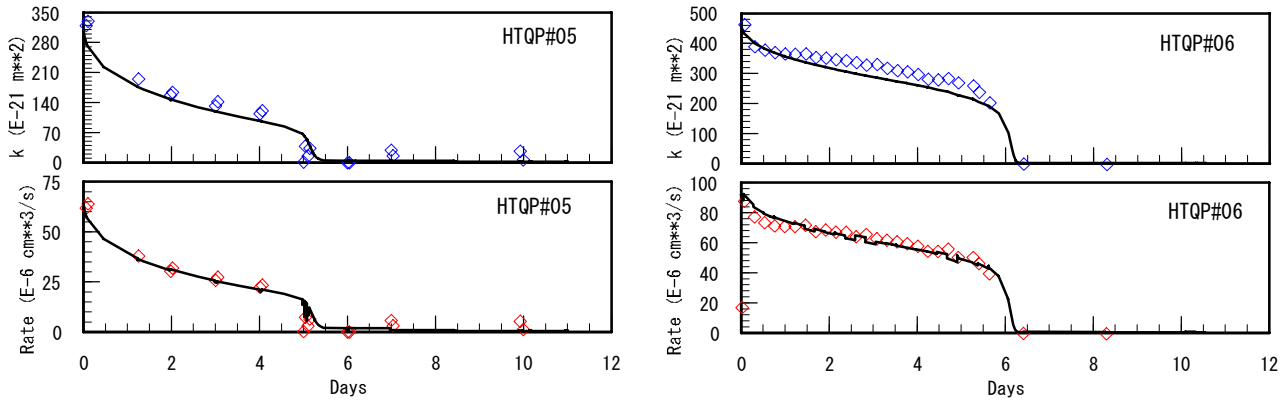

Fig. 7: Comparison between measured (symbols) and calculated (line) permeability and flowrate of intact granite at T=500º C.

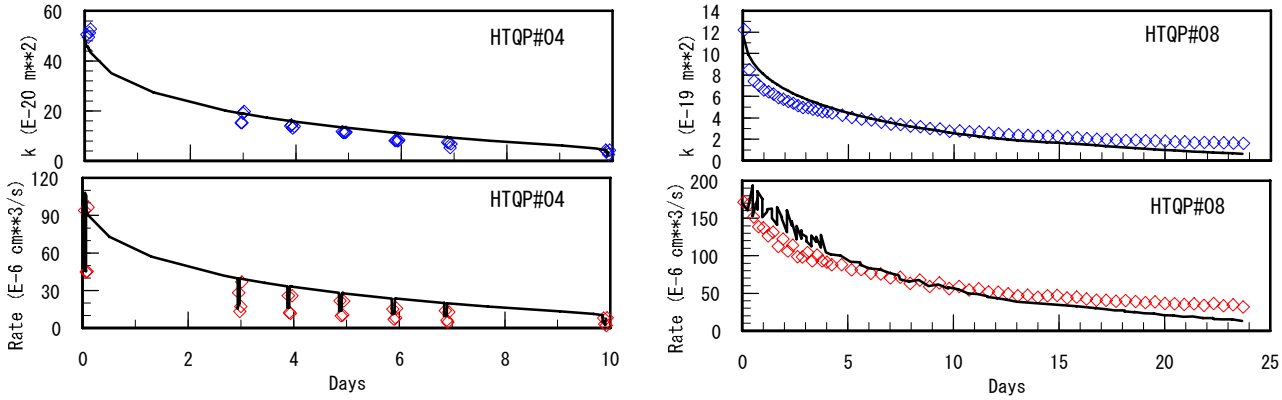

Fig. 8: Comparison between measured (symbols) and calculated (line) permeability and flowrate of granite gouge.